

Crystal Structure of Tryptophanase

Michail N. Isupov^{1*}, Alfred A. Antson², Eleanor J. Dodson²
G. Guy Dodson², Irene S. Dementieva³, Lyudmila N. Zakomirdina³
Keith S. Wilson^{2,4}, Zbigniew Dauter^{2,4}, Andrey A. Lebedev¹
and Emil H. Harutyunyan^{1*}

¹*Shubnikov Institute of Crystallography, Russian Academy of Sciences Leninsky pr. 59, Moscow 117333, Russia*

²*Department of Chemistry University of York, Heslington York YO1 5DD, UK*

³*Engelhardt Institute of Molecular Biology, Russian Academy of Sciences, Vavilov Street 32, Moscow 117984, Russia*

⁴*European Molecular Biology Laboratory, Notkestrasse 85 Geb. 25A 22603 Hamburg Germany*

The X-ray structure of tryptophanase (Tnase) reveals the interactions responsible for binding of the pyridoxal 5'-phosphate (PLP) and atomic details of the K⁺ binding site essential for catalysis. The structure of holo Tnase from *Proteus vulgaris* (space group $P2_12_12_1$ with $a = 115.0$ Å, $b = 118.2$ Å, $c = 153.7$ Å) has been determined at 2.1 Å resolution by molecular replacement using tyrosine phenol-lyase (TPL) coordinates. The final model of Tnase, refined to an R -factor of 18.7%, ($R_{\text{free}} = 22.8\%$) suggests that the PLP-enzyme form observed in the structure is a ketoenamine. PLP is bound in a cleft formed by both the small and large domains of one subunit and the large domain of the adjacent subunit in the so-called "catalytic" dimer. The K⁺ cations are located on the interface of the subunits in the dimer. The structure of the catalytic dimer and mode of PLP binding in Tnase resemble those found in aspartate aminotransferase, TPL, ω -amino acid pyruvate aminotransferase, dialkylglycine decarboxylase (DGD), cystathionine β -lyase and ornithine decarboxylase. No structural similarity has been detected between Tnase and the β_2 dimer of tryptophan synthase which catalyses the same β -replacement reaction. The single monovalent cation binding site of Tnase is similar to that of TPL, but differs from either of those in DGD.

© 1998 Academic Press Limited

Keywords: tryptophan indole-lyase; pyridoxal 5'-phosphate; protein crystallography; enzyme structure; monovalent cation binding site

*Corresponding authors

Introduction

Pyridoxal 5'-phosphate (PLP, vitamin B₆) -dependent enzymes catalyse many important reactions in amino acid metabolism, including transamination, α - and β -decarboxylation, α,β -elimination, γ -elimination, β -replacement and racemisation. According to the general mechanism for PLP catalysis proposed by Braunstein and Shemyakin

(1953) and Metzler *et al.* (1954) the reactions catalysed by PLP-dependent enzymes proceed through several common steps. These include formation of an external aldimine between the C4' of PLP and the α -amino group of the substrate and a carbanion quinonoid intermediate (Figure 1). Dunathan (1966) suggested that at the external aldimine stage of the reaction, PLP-dependent enzymes orient the scissile C α bond perpendicular to the plane of the pyridoxal imine system, thus maximising orbital overlap in the transition state and stabilising the resulting carbanion. Ivanov and Karpeisky (1969) suggested that conditions for optimal operation at each of the sequential steps of reaction catalysed by PLP-dependent enzymes are provided by structural rearrangements occurring in a preceding step. These rearrangements involve the reorientation of the pyridine ring of PLP.

X-ray crystallographic studies have been carried out on a number of α_2 dimeric aspartate aminotransferases (AATases) from different sources:

Present address: M. N. Isupov, Departments of Chemistry and Biological Sciences, University of Exeter, Exeter EX4 4QD, UK.

Abbreviations used: Tnase, tryptophanase; TPL, tyrosine phenol-lyase; PLP, pyridoxal 5'-phosphate; AATase, aspartate aminotransferase; APT, ω -amino acid pyruvate aminotransferase; DGD, dialkylglycine decarboxylase; CBL, cystathionine β -lyase; OrnDC, ornithine decarboxylase; H-bond, hydrogen bond; 3-D, three-dimensional; NCS, non-crystallographic symmetry; MR, molecular replacement; F_o , observed structure factors; F_c , calculated structure factors.

which inhibits Tnase activity (Morino & Snell, 1967), the absorption remains at 420 nm throughout the pH range 6 to 9. Various coenzyme-substrate intermediates have been identified by characteristic absorption and circular dichroic spectra (Watanabe & Snell, 1977; Zakomirdina *et al.*, 1988; Metzler *et al.*, 1991; Phillips, 1991). With many substrates and with some competitive inhibitors, the 500 nm band of the quinonoid form is produced in the presence of K^+ or NH_4^+ , but not in the presence of Na^+ (Snell, 1975; June *et al.*, 1981b; Zakomirdina *et al.*, 1988).

The most extensively studied Tnase is that of *E. coli* (comprehensive references are given by Snell, 1975; Miles, 1986; Phillips *et al.*, 1991; Metzler *et al.*, 1991). Some physical and biochemical properties of *P. vulgaris* Tnase were deduced by De Moss and Mozer (1969) and Simard *et al.* (1975a,b). The Tnase from *P. vulgaris* is a tetramer of 52 kDa subunits each made up of 467 residues (Kamath & Yanofsky, 1992). Each subunit contains one molecule of PLP which forms a Schiff's base with the ϵ -amino group of Lys266 (Kamath & Yanofsky, 1992).

The primary structures of Tnases from two strains of *E. coli* (Deeley & Yanofsky, 1981; Tokushige *et al.*, 1989), *P. vulgaris* (Kamath & Yanofsky, 1992), *S. thermophilum* (Hirahara *et al.*, 1992) and *Enterobacter aerogenes* SM-18 (Kawasaki *et al.*, 1993) have been determined. The Tnase amino acid sequences exhibit an identity in the range 50% to 60%. Another α,β -eliminating PLP-dependent lyase, TPL, has high level of sequence homology with Tnase (Kamath & Yanofsky, 1992). Sequences of TPL from *Citrobacter freundii* (Iwamori *et al.*, 1991; Antson *et al.*, 1993) and Tnase from *P. vulgaris* have 50% identity.

Although biochemical studies of Tnase have been underway for many years, X-ray structural investigations were prevented by difficulties in crystallising the enzyme. The first crystals of the *E. coli* enzyme suitable for X-ray study were reported in 1991 (Kawata *et al.*). Recently we described the crystallisation and preliminary X-ray investigation of Tnases from *E. coli* and *P. vulgaris* (Dementieva *et al.*, 1994). Here we present the crystal structure of holo Tnase from *P. vulgaris* refined at 2.1 Å resolution.

Results and Discussion

Quality of the final model

Tnase has been refined to an R -factor of 18.7% for all data without σ cutoff in the resolution range 18 to 2.1 Å excluding 2.0% randomly distributed reflections assigned to calculate R_{free} 22.8%, (Table 1). The asymmetric unit contains an α_4 Tnase tetramer. The final electron density allowed the positioning of residues 2 to 466 out of the total 467 residues for all four subunits. The model contains four PLP molecules, four potassium ions and 941 water molecules. The dispersion precision indi-

Table 1. Model refinement statistics

Resolution range (Å)	18.0–2.1
$R_{cryst} = \Sigma F_o - F_c / \Sigma F_o $	18.7%
No. of reflections in refinement	115,498
R_{free}	22.8%
No. of reflections used for R_{free}	2364 (2% of total)
No. of protein atoms	14,772
No. of coenzyme atoms and metal ions	64
No. of water molecules	941
Average B -factor for protein atoms (Å ²)	27.7
Average B -factor for solvent molecules (Å ²)	31.8
rms deviations from ideality (target values are given in parentheses)	
Bond lengths (Å)	0.012 (0.020)
Bond angles (Å)	0.030 (0.040)
1–4 neighbours (Å)	0.034 (0.050)
Planar groups (Å)	0.021 (0.020)
Chiral volumes (Å ³)	0.118 (0.150)
Torsion angles (deg.)	
Planar	4.1 (7.0)
Staggered	17.8 (15.00)
Orthonormal	27.2 (20.00)
B -factors correlation (Å ²)	
Main-chain bond	2.8 (4.0)
Main-chain angle	3.7 (6.0)
Side-chain bond	5.7 (8.0)
Side-chain angle	7.7 (10.0)

cator (Cruickshank, 1996; Murshudov & Dodson, 1997) gives an overall estimate of rms error in coordinates of 0.16 Å for the well-defined part of the structure. The average main-chain atom B -factors for one subunit are shown in Figure 2. The overall G -factor calculated by PROCHECK (Laskowski *et al.*, 1993, 1994) as a measure of the stereochemical quality of the model is 0.0 which is better than expected at 2.1 Å resolution. Of the non-glycine residues, 90.7% fall in the most favoured regions of Ramachandran plot (Ramakrishnan & Ramachandran, 1965; Figure 3). Five residues in each subunit are in the left-handed helical conformation. The rms deviation of peptide units from planarity is 4.1°. Ile192 and Pro249 in each subunit are in the *cis*-conformation. About 39% of the amino acids are in α -helices, 21% in β -sheets and 18% in β -turns or 3_{10} helices. Two residues in each subunit, Pro8 ($\phi = -85.3^\circ$, $\psi = 34.8^\circ$) and the PLP binding Lys266 ($\phi = -109^\circ$, $\psi = -108^\circ$), have unfavourable main chain torsion angles. However the electron density for these two residues is unambiguous and their B -factors are low.

The structure factors and refined coordinates of Tnase have been deposited with the Brookhaven Protein Data Bank (Bernstein *et al.*, 1977); the access code is 1ax4.

Description of the structure

The Tnase monomer (Figure 4(a) and (b)) is composed of an N-terminal arm (residues 1 to 19) and two α/β domains. The small domain is formed by residues 20 to 51 and 323 to 467, the large domain includes residues 60 to 319. Residues 51 to 60 and 319 to 322 form interdomain regions. The assign-

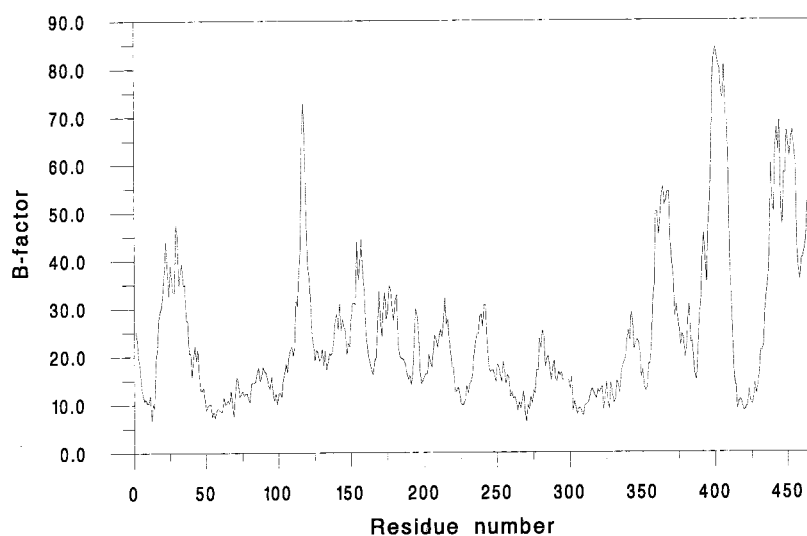


Figure 2. Average temperature factors (\AA^2) for main-chain atoms of one of Tnase subunits as a function of residue number.

ment of Tnase secondary structural elements is shown in Figure 5.

The small domain has a four-stranded ($\beta A'$, $\beta B'$, $\beta C'$ and $\beta D'$) antiparallel β -sheet with $+1, +2x, -1$ topology (Richardson, 1981; Figure 6(a)). One side of the β -sheet forms the interdomain interface with the large domain. The other side is covered by four α -helices which are accessible by solvent. In addition, a β -hairpin formed by residues 446 to 451 and 462 to 466 is located near the C terminus of the small domain. The N-terminal part of the small domain is con-

nected with the C-terminal by residues 45 to 47 which form a parallel β -bridge, βI , with strand $\beta C'$ and make an additional hydrogen bond with strand $\beta D'$. The core of the large domain is a seven-stranded β -sheet ((βA , βG , βF , βE , βD , βb and βC , Figure 6(b)) of a mixed type with topology $+5x, +1x, -2x, -1x, -1x, -1$ and direction $+ - + + + + +$. The large domain β -sheet is surrounded by three α -helices on the side adjacent to the small domain and six α -helices on the outer side. The PLP is located in the interdomain cleft and is also coordinated by residues from a neigh-

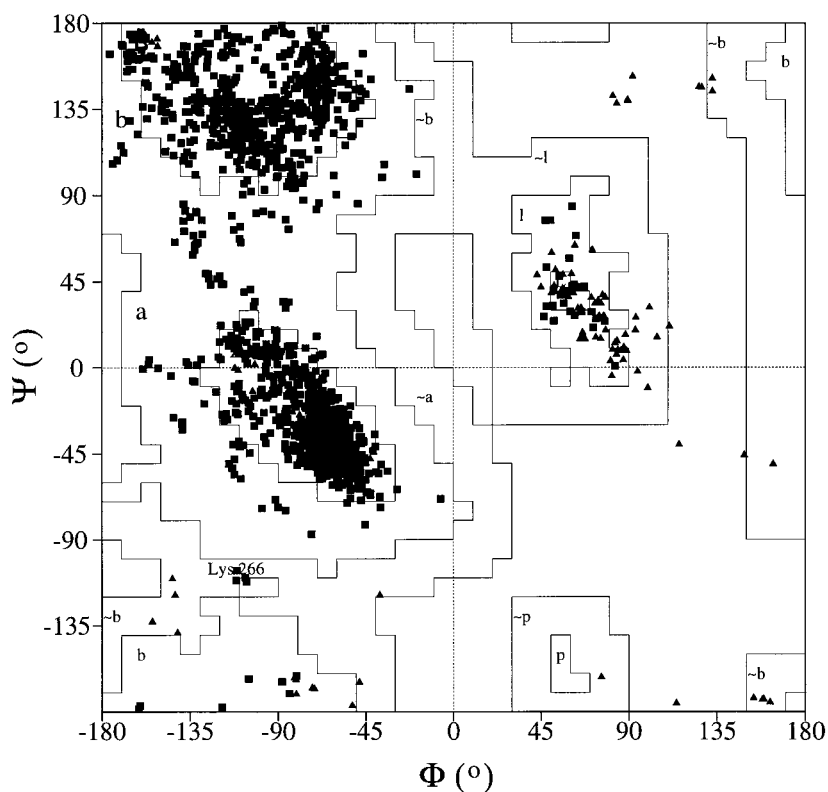


Figure 3. The Ramachandran (ϕ, ψ) plot for four crystallographically independent subunits of Tnase. Glycine residues are represented by triangles.

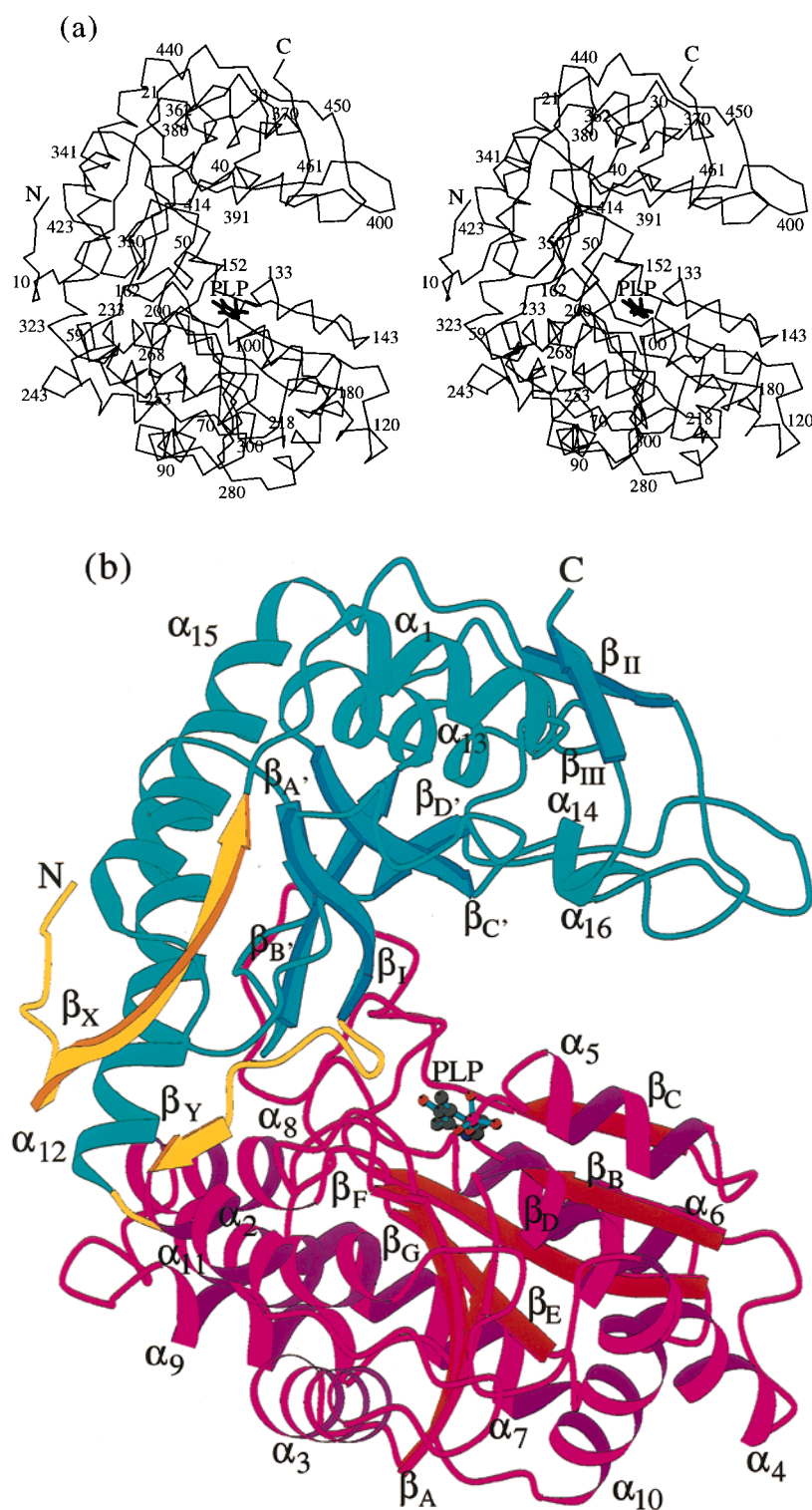


Figure 4. Folding of the Tnase subunit. (a) Stereo view of the C α trace. Each 20th residue is numbered. (b) Ribbon diagram of the subunit in the same orientation as in (a). Small domain is shown in blue, large domain in red, N terminus and intersubunit regions in yellow. The figure was generated by MOLSCRIPT (Kraulis, 1991)

bouring subunit. These two subunits associate tightly to form a dimer resembling the AATase dimer (Kirsch *et al.*, 1984). The active sites of Tnase are formed by residues from both subunits in this dimer. This dimer will henceforth be referred to as the "catalytic" dimer (Figure 7). The monovalent cations are located on its intersubunit interface. The network of hydrogen bonds and salt bridges formed on the intersubunit interface upon binding

of the PLP and monovalent cations contribute to the stability of the catalytic dimer. The side-chains of His98, Asp105 and Met295 make contacts with their symmetry equivalents in the catalytic dimer.

The overall size of Tnase tetramer is about 105 Å × 80 Å × 60 Å. It comprises two catalytic dimers and has 222 point group symmetry (Figure 8(a) and (b)). The centres of mass of the subunits form a flat orthorhombic tetrahedron



Figure 5. Secondary structure and amino acid sequence of Tnase from *P. vulgaris* (Kamath & Yanofsky, 1992) shown in the one letter code. The α -helices, β -strands, 3_{10} helices and β -turns are indicated by the labels (H), (S), (G) and (T), respectively. The numbering of β -strands is the same as in the secondary structure of TPL (Antson *et al.*, 1993). Amino acid residues shown in bold type are conserved in all known Tnase and TPL sequences including Tnases from *P. vulgaris*, *E. coli*, *E. aerogenes*, *S. thermophilum*, *Proteus inconstans* (Hirahara *et al.*, 1993) and TPLs from *C. freundii*, *Erwinia herbicola* (Iwamori *et al.*, 1992), *Symbiobacterium thermophilum* (Hirahara *et al.*, 1993). Residues that are invariant in the Tnase sequences only, are underlined. The alignment of Tnase and TPL sequences was performed by the GCG package (GCG, 1994).

with edges 36.1 Å, 46.8 Å and 58.1 Å, in agreement with electron microscopy studies (Morino & Snell, 1967). All three molecular dyads in the tetramer are non-crystallographic and are named *P*, *Q*, *R* in accordance with the nomenclature suggested for TPL (Antson *et al.*, 1993; Figure 8(a)). The subunits in the catalytic dimer are related by the molecular dyad *Q*. The N-terminal "arms" of two subunits related by the *R* molecular axis intertwine and are involved in the intersubunit β -sheet (β XA, β YC, β YA and β XC; Figure 6(c)). The side-chains of Arg4 and Ile66 make contacts with their symmetry equivalents across this axis. The subunits of the tetramer related by the *P* molecular dyad have the

loosest association, mainly through hydrophobic interactions *via* residues from helices α_2 .

A four helix bundle is formed at the centre of the tetramer by helix α_2 (59 to 67) from each subunit. The axes of the two helices from subunits related by the *P*-axis are parallel and lie at an angle of about 30° to the axes of the other pair of helices. Residues Trp62 and Ile66 on these helices together with Met57 and Met13 from all four subunits form a hydrophobic cluster at the centre of the tetramer, (Figure 9), which contributes to its stability. None of the residues in this hydrophobic cluster are conserved among other Tnase and TPL sequences.

It has been shown (Gopinatham & DeMoss, 1966) that the *E. coli* apo Tnase tetramer dissociates into dimers at low pH or temperature, while the holo form of enzyme does not. Monovalent cations also influence the stability of the apo Tnase tetramer (Snell, 1975). Morino & Snell (1967) concluded from measurements of thermodynamic parameters for dissociation of apo Tnase from tetramer to dimers that both hydrophobic and ionic forces are important for maintaining the quaternary structure. As seen from the Tnase structure, both PLP and the monovalent cations contribute to the stability of the catalytic dimer and in their absence the tetramer of apo Tnase might well dissociate into two dimers each formed by a pair of subunits related by the *R* molecular dyad (Figure 8(a)).

The large domains of all four Tnase subunits superimpose with an r.m.s. deviation between their C α atom positions of only 0.06 to 0.07 Å. Such high similarity may result from the use of NCS restraints during refinement (see Materials and Methods). However the C α atoms of the complete subunits superimpose with an rms deviation of 0.25 to 0.55 Å. When the whole subunits are superimposed using all atoms of the large domains, the difference in main chain positions for some parts of the small domain is as much as 3 Å with the direction of displacement toward the large domain (Figure 10). For helices α_1 and α_{13} , which are in well-defined electron density, the deviation in C α positions is 1.2 to 1.7 Å. An attempt to impose strict NCS restraints for the small domains of all four subunits during refinement resulted in an increase of both *R*-factor and *R*_{free}.

Active site

The active site is located near the subunit interface in the catalytic dimer (Figure 7). A catalytic cleft is formed by the large and small domains of one subunit and the large domain of the neighbouring subunit. PLP is located at the bottom of the catalytic cleft and is tightly bound to the protein at the C-terminal end of the large domain β -sheet through several specific interactions mainly with residues from the large domain (Figure 11).

The continuous electron density from Lys266 NZ to PLP C4' confirms the presence of the internal aldimine form of the cofactor in all four subunits (Figure 12). The double bond Lys266 NZ-PLP C4'

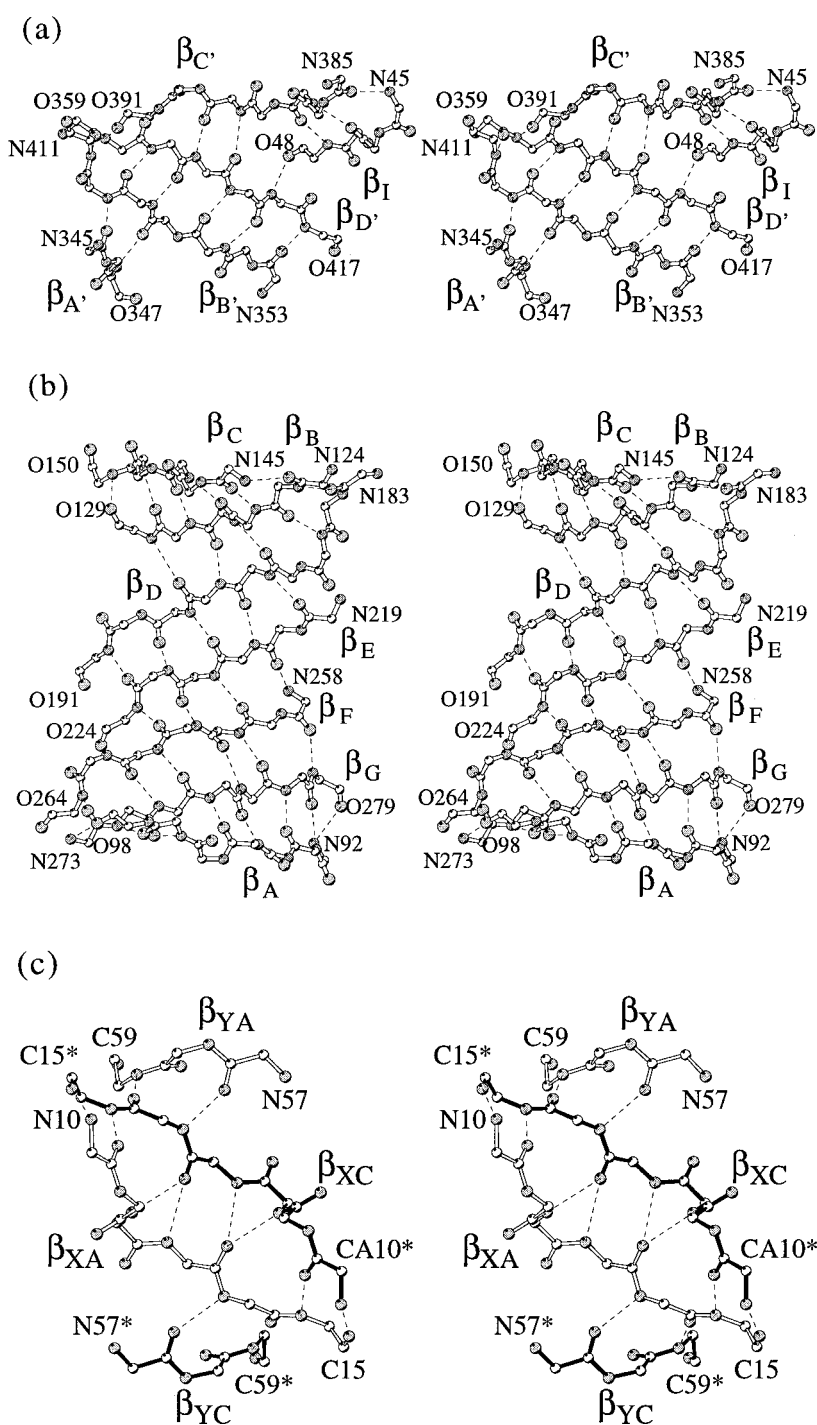


Figure 6. Stereo plot of the main-chain atoms of the β -sheets of Tnase generated by MOLSCRIPT (Kraulis, 1991). Residues at the ends of each β -strand are labelled. Hydrogen bonds are shown by dashed lines. (a) Four-stranded β -sheet of the small domain, as seen from outside looking towards the large domain. The order of strands from top to bottom is $\beta_{C'}$, $\beta_{D'}$, $\beta_{B'}$ and $\beta_{A'}$. Residues 45 to 48 which form the β -bridge are also shown. (b) the β -Sheet in the large domain as seen from the small domain. The order of strands from top to bottom is β_C , β_B , β_D , β_E , β_F , β_G and β_A . (c) Intersubunit β -sheet, viewed along the molecular dyad R. The lower subunit (C) is shown by filled bonds, the upper subunit (A) is shown by open bonds. Two β -strands from each subunit, β_X and β_Y contribute to the β -sheet. The residues from subunit C are marked with an asterisk. The order of strands from top to bottom is β_{YA} , β_{XC} , β_{XA} and β_{YC} .

is not coplanar with the PLP pyridine ring, but tilted by about 30° , causing displacement of Lys266 NZ by 0.7 \AA out of the pyridine ring plane. Lys266 is orientated to the *si* face of the coenzyme. The aldimine linkage is directed towards PLP O3' and its imine nitrogen makes a hydrogen bond/salt bridge with it. PLP O3' also forms a salt bridge with Arg226 NH1. Asn194 ND2 could have formed a hydrogen bond with PLP O3', but this would require a rotation of 90° around its C β -C γ bond. Asp223 OD2 makes a salt bridge with the protonated N1 atom of the PLP pyridine ring. Asp223

OD1 makes H-bonds with Ser224 N and Ala225 N. Asp223 OD2 is H-bonded to Thr135 OG1.

The PLP pyridine ring is sandwiched between Ala225 from protein side and the aromatic ring of Phe132 (Figure 11) from the solution side, the latter being tilted by about 30° with respect to the plane of the pyridine ring. The PLP phosphate group is located near the N terminus of helix α_4 (100 to 118) and stabilised by its dipole. The negative charge of the phosphate is partially compensated by a salt bridge with the guanidinium group of Arg101. The phosphate moiety makes H-bonds with Gly100 N



Figure 7. Stereo diagram of the C^α trace of the two Tnase subunits forming the catalytic dimer viewed along non crystallographic dyad Q. View from the top of the molecule toward the centre. The subunits are shown with different linewidths. Potassium ions are represented by filled circles, PLP molecules are shown in thick bonds. The figure was generated by MOLSCRIPT (Kraulis, 1991).

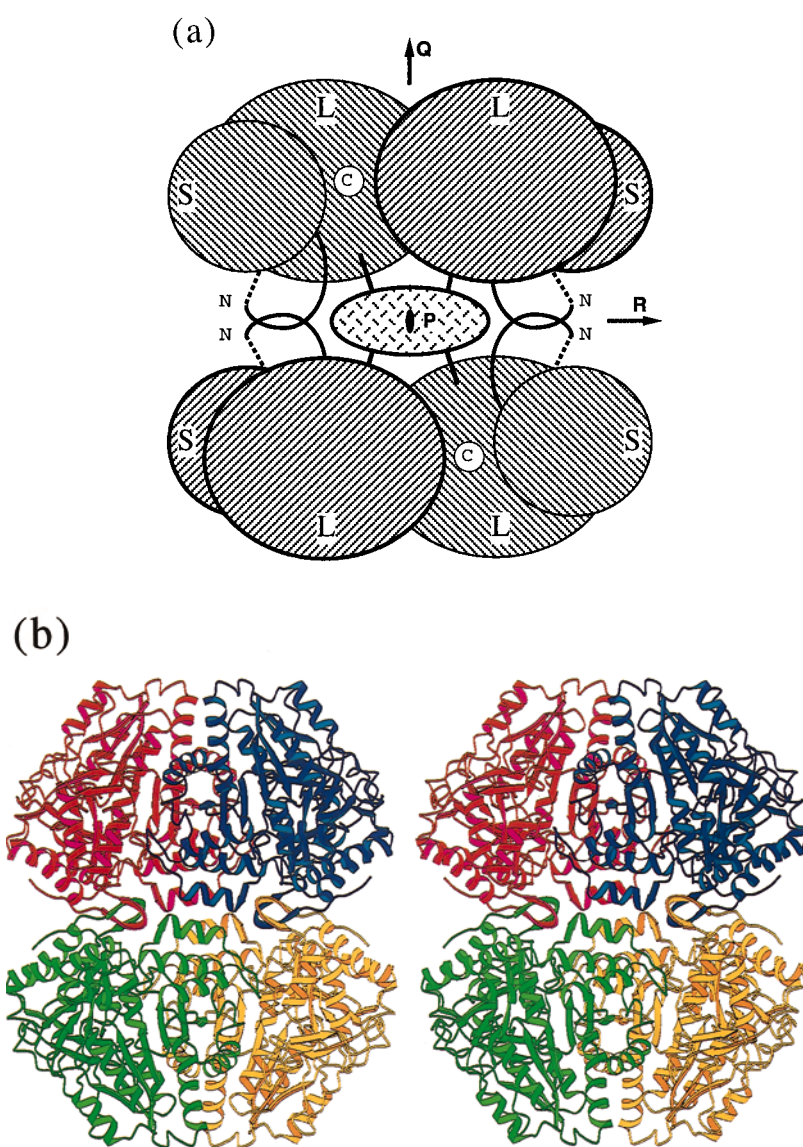


Figure 8. The Tnase tetramer (a) Schematic representation of the domain architecture and intersubunit contacts in Tnase, viewed along the molecular dyad P with the molecular dyad Q vertical. Large domains are marked as L , small domains as S , the catalytic cleft is marked as C and the N termini are marked N . The hydrophobic cluster is shown as an ellipsoid in the centre of the molecule. (b) Ribbon stereodiagram of the Tnase tetramer viewed as in (a). Different subunits are shown in different colours. The figure was generated by MOLSCRIPT (Kraulis, 1991).

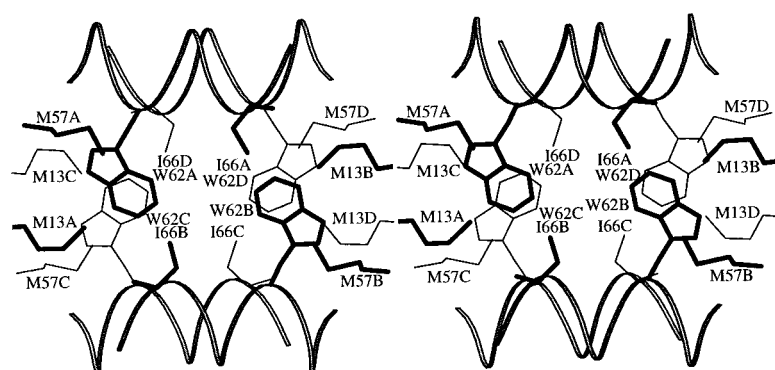


Figure 9. Stereo plot of the four α -helix bundle and hydrophobic cluster viewed along the molecular dyad Q (Figure 8). α -Helices are shown as thin ribbons, the residues from different catalytic dimers are shown with different line width. The figure was generated by MOLSCRIPT (Kraulis, 1991). Residue number is followed by name of subunit to which it belongs.

and Arg101 N, Gln99 NE2 and Ser263 OG. In addition, Ser52 OG, Lys265 NZ, Tyr72 OH and Tyr301 OH are H-bonded to water molecules which coordinate the phosphate group. Tyr72 and Tyr301 belong to the adjacent subunit in the catalytic dimer. Schnackerts & Snell (1983) showed by ^{31}P NMR that the PLP phosphate group in *E. coli* holo Tnase is in the dianionic form throughout the pH range 5.8 to 8.2. They suggested that a salt bridge with a positively charged protein group was responsible for the lowering of the pK of the PLP phosphate. From the present Tnase structure it seems that the guanidinium group of Arg101 plays such a role.

The B-factors of the PLP atoms are close to those of the surrounding protein, essentially suggesting full occupancy of the PLP sites. The electron density is quite clear (Figure 12) and suggests a single conformation of PLP in the active site. There are several possible forms of internal aldimine PLP-enzyme in *E. coli* Tnase in the presence of activating K^+ (June *et al.*, 1981a; Metzler *et al.*, 1991). One

is the ketoenamine with a protonated aldimine N and deprotonated PLP O3' (Figure 13(a)) which has an absorption peak at 420 nm. Another one is an enolimine form (June *et al.*, 1981a) with protonated PLP O3' and deprotonated aldimine N (Figure 13(b)) which absorbs at 337 nm. A species with an absorption band at 355 nm has been detected by scanning stopped flow spectrophotometry in conditions of pH jump and pH drop (June *et al.*, 1981a) and resolution of absorption spectra with lognormal curves (Metzler *et al.*, 1991). June *et al.* (1981a) attributed this band to the dipolar ionic ring species (Figure 13(c)) in which aldimine N is deprotonated, PLP N1 protonated and PLP O3' deprotonated. An alternative structure has been proposed for the 337 nm form, namely an adduct in which a deprotonated nucleophilic group Y or a hydroxyl ion is added to the C4' (O'Leary & Brummond, 1974; Figure 13(d)). The 420 nm form predominates at low pH or in the absence of activating monovalent cations. In the presence of these cations the percentage of the

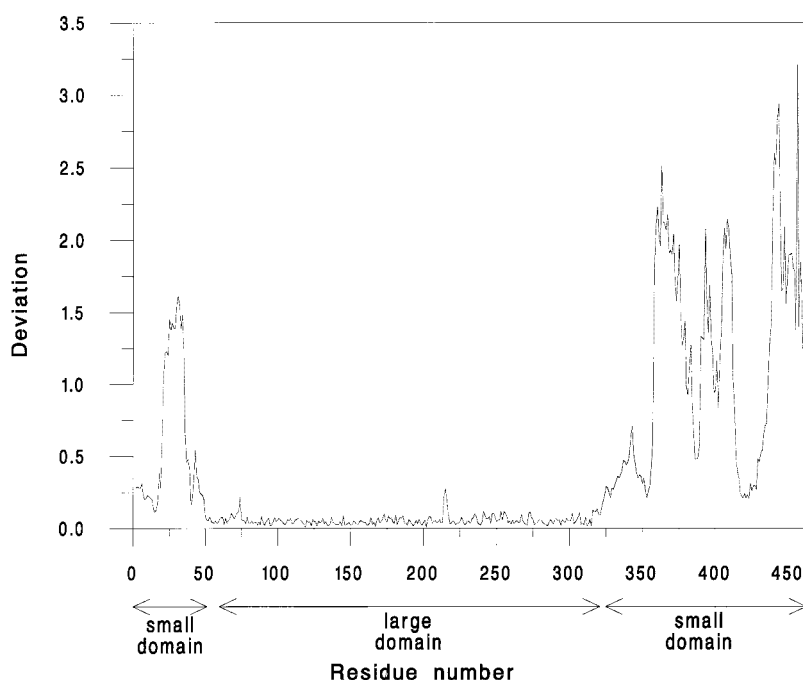


Figure 10. Deviation (in Å) of C^α atom positions between the two Tnase subunits (A and B) when superimposed by atoms of large domain only.

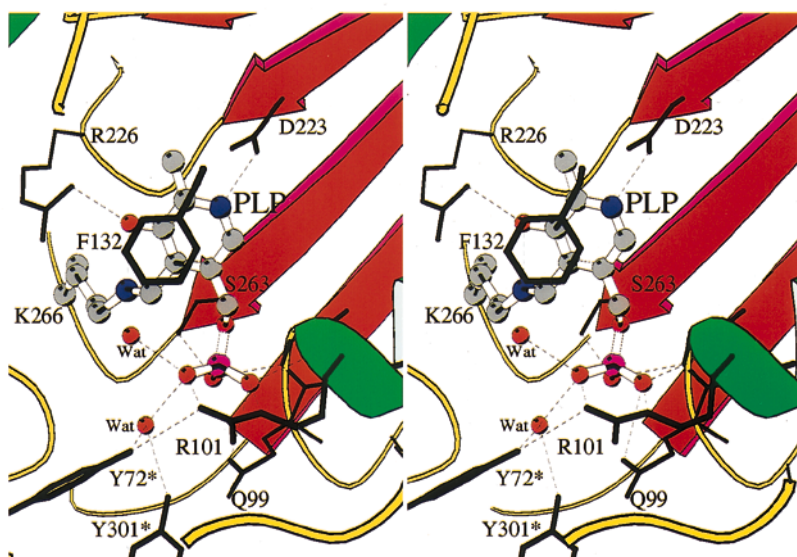


Figure 11. Cofactor-protein interactions in the active site of Tnase. The view is from the outside toward the β -sheet of the large domain. Helix α 5 covering PLP from the solution side is not shown. Hydrogen bonds are shown by broken lines. Located in the centre of the figure, PLP lies near the C termini of β -strands β E and β F of the large domain. It is covalently bound to Lys266 through an imine linkage NZ-C4'. PLP and the side-chain of Lys266 are shown as ball and stick models. The phosphate group of PLP is located near N terminus of helix α 4. Residues that participate in binding of the coenzyme are labelled and shown as filled bonds. Residues from adjacent subunit are marked by an asterisk. Figure was generated by MOLSCRIPT (Kraulis, 1991).

337 nm form rises with increasing pH. Absorption spectra of *P.vulgaris* Tnase (Simard *et al.*, 1975b) show that at pH 7.8 at which the crystals were obtained there is an equilibrium between the 420 and 337 nm absorbing species.

In the crystal structure of Tnase there is a salt bridge between the positively charged guanidinium group of Arg226 and PLP O3' in Tnase. This strongly suggests that PLP O3' is deprotonated. PLP C4' is not covalently bound to any protein group other than Lys266 and there is no additional $F_o - F_c$ density at C4' to indicate the presence of an additional substituent. This implies that the ketoenamine species (Figure 13(a)) prevails in the structure. The existence of a salt bridge Asp223 OD2 to PLP N1 favours protonation of the pyridine ring.

The absence of other species observed in the active site of the Tnase crystal structure requires

additional discussion. If 337 nm form is enolimine (Figure 13(b)), structural rearrangements in the active site are required to provide reorientation of the PLP and to break its salt bridges with Arg226 and Asp223, which probably involve domain movement. This is supported by the fact that 420 nm form undergoes fast transaldimination in the presence of substrate, while 337 nm form has a lag period (June *et al.*, 1981b; Metzler *et al.*, 1991). It seems plausible that crystal packing affects the domain movement and thus shifts the equilibrium between 337 and 420 nm species in favour of ketoenamine.

If, however the 337 nm form is not enolimine but the so called "alternative" form with OH adduct at imine nitrogen (O'Leary & Brummond, 1973; Figure 13(d)), certain amounts of these species could be present in the active site unde-

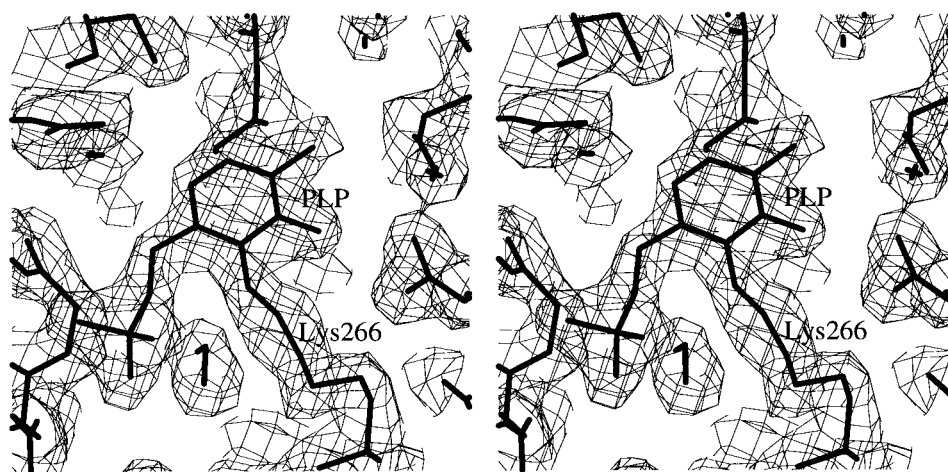


Figure 12. Stereo drawing showing the averaged electron density map around the cofactor binding site. Electron density map was calculated using data in the resolution range 10 to 2.1 Å and contoured at 1 rms. The continuous density for bond Lys266 NZ-PLP C4' illustrates the Schiff's base linkage. Produced using the program O (Jones *et al.*, 1991).

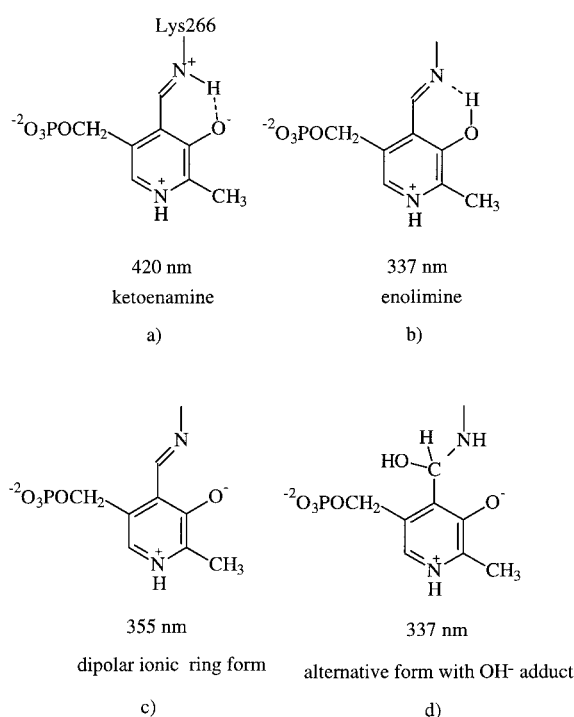


Figure 13. Scheme showing proposed ionisation states of the PLP-enzyme internal aldimine species in the active site of Tnase at pH 7.8 at which the crystals were grown (June *et al.*, 1981a; Metzler *et al.*, 1991). (a) Ketoenamine form with absorption maximum at 420 nm. (b) Enolimine form with absorption maximum at 337 nm. (c) Dipolar ionic ring form with absorption maximum at 355 nm. (d) Alternative structure for the 337 nm form, an adduct in which H₂O or another nucleophile is added at position C4' of the ketoenamine.

tected due to the limited resolution of Tnase X-ray data (2.1 Å). A water molecule lying at 2.9 Å distance from C4' and H-bonded to PLP phosphate group in the Tnase crystal structure (Figure 11) could serve as a nucleophile which attacks ketoenamine C4' from the *re* side of PLP ring to form this adduct. However the possibility of the 337 nm species being the alternative form seems quite remote and the candidate water discussed simply occupies the position from which the substrate α -amino group attacks internal aldimine to form external aldimine (Figure 1).

Cys298 in *E. coli* Tnase has been proposed to be in, or close to the active site by Phillips and Gollnick (1989) but not to be involved in catalytic activity. The Cys298Ser *E. coli* Tnase mutant exhibits reduced affinity for PLP ($K_{CO} = 6 \mu\text{M}$ instead of 1.5 μM for wild-type; Phillips & Gollnick, 1989). The apo Tnase of *E. coli* is inactivated by bromopyruvic acid, while the Cys298Ser mutant *E. coli* apo enzyme is resistant to such inactivation (Phillips & Gollnick, 1989). Cys292 in Tnase from *P. vulgaris*, equivalent to Cys298 in *E. coli* Tnase, is located about 7 Å from the phosphate group of PLP, bound to the adjacent subunit in the catalytic

dimer. Cys292 determines the conformation of loop 296 to 303 through interactions of its side-chain. When the enzyme binds PLP the guanidinium group of Arg101, which makes a salt bridge with the cofactor phosphate, also forms an H-bond with Thr297 O lowering the solvent accessibility of the Cys292 side-chain. Thus PLP binding to *E. coli* Tnase prevents chemical modification of Cys298. The lowered affinity of the Cys298Ser *E. coli* Tnase mutant for PLP can be explained by unfavourable interactions of Ser298 OG in this hydrophobic environment, affecting the conformation of the side-chain of Arg103 (Arg101 in Tnase of *P. vulgaris*) and making its salt bridge with the co-factor phosphate less favourable.

The description of the substrate binding site has to await structures of Tnase complexes with substrate analogues. However, the most probable candidate for the substrate α -carboxylate binding residue is Arg414 which is conserved in all Tnase and TPL sequences. The corresponding Arg404 binds α -carboxylate of the substrate analogue 3-(4-hydroxyphenyl) propionate α -carboxylate in TPL (Antson *et al.*, 1994).

Monovalent cation binding sites

When solvent was being incorporated into the Tnase structure, all strong positive peaks in the ($F_o - F_c$) maps were initially described as water molecules. After partial refinement, four water molecules had *B*-factors of about 2 Å², much lower than the *B*-factors of surrounding protein atoms (10 to 15 Å²). Large positive peaks were visible in the ($F_o - F_c$) synthesis at these sites, indicating high atomic number atoms. The peaks occupied the same position on the catalytic dimer interface in all four subunits and had only carbonyl and carboxyl enzyme groups in the first coordination sphere. As the mother liquor contained 0.1 M Cs⁺ and 0.1 M K⁺ and no divalent metal ions, the peaks were described as K⁺. When K⁺ were introduced at these sites, the *B*-factors were comparable to those of the surrounding protein atoms, suggesting that the ions are indeed K⁺ and that any Cs⁺ substitution is small, in keeping with the much higher affinity of *E. coli* Tnase for K⁺ ($K_A = 1.44 \text{ mM}$) than for Cs⁺ ($K_A = 14.6 \text{ mM}$) (Suelter & Snell, 1977). This identification of one monovalent cation binding site per subunit is consistent with the hyperbolic saturation curve of monovalent cation activation of Tnase in excess of substrate (Suelter & Snell, 1977), but contradicts the two monovalent cations per subunit suggested by equilibrium dialysis studies of TI⁺ binding (Suelter & Snell, 1977).

The monovalent cation binding sites are located at the intersubunit interface in the catalytic dimer (Figure 7). The coordination sphere of the K⁺ includes Gly53 O and Asn271 O from one subunit, Glu70 OE1 and Glu70 O from the second subunit in the catalytic dimer and three water molecules (Figure 14). Gly53 is located in the β -turn on the

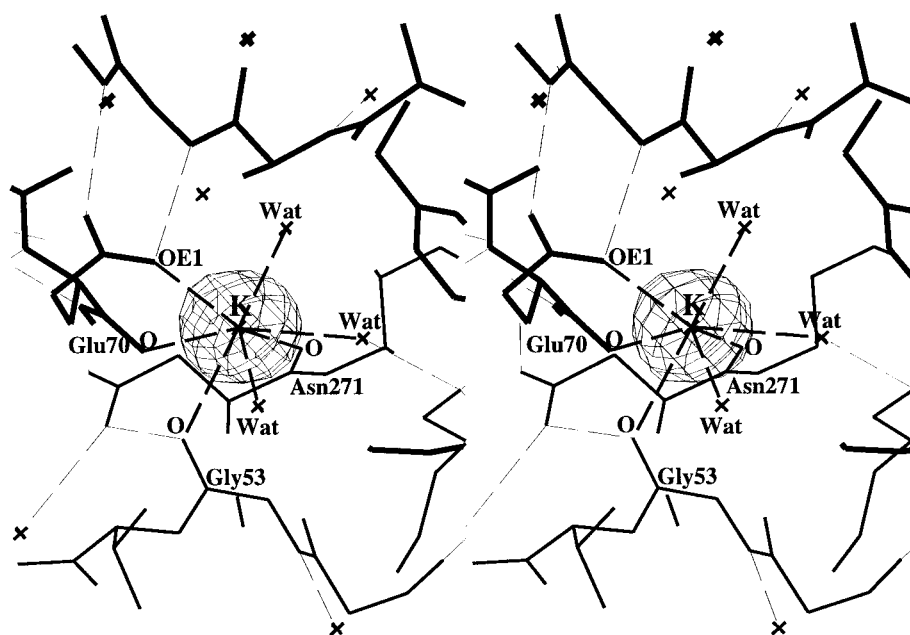


Figure 14. Stereo drawing of the K^+ binding site of Tnase at the subunit interface in the catalytic dimer. ($F_o - F_{ck}$) omit electron density map is shown contoured at 5 rms level, where F_{ck} were calculated from the model with K^+ occupancies set to 0. Residues involved in monovalent cation coordination are labelled. The subunits of catalytic dimer are shown in different line width. Hydrogen bonds are shown by broken lines. The figure was made using QUANTA (Molecular Simulations).

connecting interdomain region. Glu70 belongs to the loop between helices $\alpha 2$ and $\alpha 3$ in the large domain. Asn271 is situated in the β -turn between βF and βG of the large domain, which is preceded by the loop 265 to 269 containing the PLP binding Lys266. Gly53 and Glu70 are conserved in all known TPL and Tnase sequences. Asn271 is also conserved in most Tnases and TPLs but is replaced by Pro in *E. coli* Tnase. The distances between K^+ and its ligands (Figure 15) are keeping with those for K^+ in cyclic organic chelators such as valinomycin and nonactin (Woehl & Dunn, 1995). As expected from electrostatic considerations the closest ligand is the carboxylate oxygen of Glu70 (2.72 Å), bonds to Gly53 and Asn271 are typical of K^+ -O bonds to carbonyl oxygen with lengths of 2.82 and 2.87 Å, respectively, as are the bonds to water (2.78, 2.85 and 2.98 Å). The ligands do not form regular pentagonal bipyramidal or octahedral structure as in case of Mg^{2+} or Ca^{2+} , rather, they are irregularly distributed around the ion. K^+ is situated about 8 Å from the nearest cofactor atom (PLP OP2). The distance from K^+ to PLP N1 is 15.5 Å and to PLP C4' 11.5 Å. The distance between the two K^+ in the catalytic dimer is 17.7 Å. The NZ of Lys265 adjacent to the PLP binding Lys266 makes H-bonds with both the water which is a ligand of the K^+ and with Gln99 OE1 while Gln99 NE2 is H-bonded to the PLP phosphate (Figure 15).

Since the discovery of the K^+ activation of pyruvate kinase (Boyer *et al.*, 1942) a large number of enzymes have been demonstrated to be specifically regulated by monovalent cations (Suelter, 1970). It

has been suggested that monovalent cations maintain a specific protein conformation necessary for optimum catalytic activity (Evans & Sorger, 1966) or are directly involved in catalysis (Melchior, 1965). Most monovalent cation dependent enzymes are activated by K^+ and NH_4^+ , but some extracellular proteins e.g. human α -thrombin show a preference for activation by Na^+ (Wells & Di Cera, 1992). To date, monovalent cations important for activity have been identified in crystal structures of rhodanese (Lijk *et al.*, 1984; Kooystra *et al.*, 1988), dialkylglycine decarboxylase (Toney *et al.*, 1993, 1995), TPL (Antson *et al.*, 1994) and tryptophan synthase (Rhee *et al.*, 1996). Although non-specific binding of Na^+ and K^+ has been found in several other proteins, they do not appear to have particular structural or functional roles.

In vivo Tnase should exist in complex with K^+ as their concentration in the cell of 150 to 200 mM (Metzler, 1977) is two orders of magnitude higher than the K_A of *E. coli* Tnase for K^+ which is 1.44 mM (Suelter & Snell, 1977). NH_4^+ , K^+ , Tl^+ or Rb^+ are required for activity of all Tnases *in vitro* and their effects are antagonised by Na^+ and Li^+ (Snell, 1975). Monovalent cations in Tnase increase the strength of intersubunit cohesion and the affinities of the apo enzymes for PLP and of holo enzymes for substrates, affect the switch from the 420 nm to the 337 nm form of the holo enzyme and are essential for labilisation of the substrate α -proton (Hogberg-Raibaud *et al.*, 1975; Snell, 1975; Suelter & Snell, 1977). Several other α,β -specific PLP-dependent enzymes require monovalent cations for activity. Similar activation by NH_4^+ or K^+

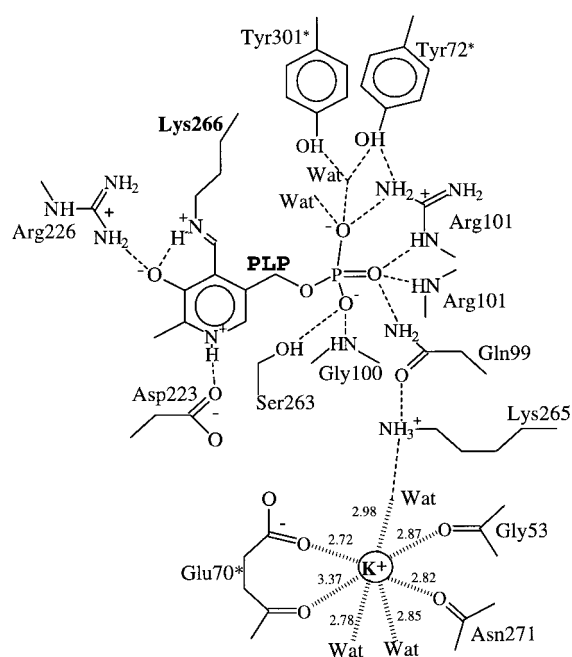


Figure 15. Schematic representation of the hydrogen bond network in the PLP-binding site and the chelate bonds of K^+ in Tnase. The ketoenamine form of holo Tnase is shown with protonated pyridinium nitrogen. Hydrogen bonds are shown by broken lines. The chelate bonds of K^+ are shown by dash-stacked lines. The cation–ligand distances (Å) are indicated. Glu70, Tyr72 and Tyr301 (marked by an asterisk) belong to the neighbouring subunit of the catalytic dimer.

and inhibition by Na^+ was observed in TPL (Toraya *et al.*, 1976; Demidkina & Myagkih, 1989), tryptophan synthase, and in threonine and D- and L-serine dehydratases (Miles, 1986).

The large distance between the PLP moiety and K^+ in Tnase excludes the possibility of direct involvement of monovalent cations in catalysis. They could, however, influence the relative position of the domains within subunit and/or conformations of certain loops providing the necessary alignment of enzyme catalytic groups at some stage of catalysis. Clarification of catalytically important conformational changes due to monovalent cation binding will require structures of holo Tnase with and without bound ions. However, some suggestions may be considered. Movement of the conserved Lys265 preceding PLP-binding Lys266 could affect orientation of PLP pyridine ring. The substitution of analogous Lys269 by Arg in *E. coli* Tnase affects formation and breakdown of quinonoid complex (Phillips *et al.*, 1991), the effect similar to that observed in the absence of monovalent cations (Hogberg-Raibaud *et al.*, 1975). Changes in the conformation of Gly53, situated in a flexible loop between small and large domains, upon monovalent cation binding could result in different relative positions of domains in the Tnase subunit.

This suggestion is supported by the fact that the sedimentation coefficient of the *E. coli* Tnase holo enzyme in high Na^+ (inactive enzyme) is lower than in high K^+ (active enzyme) (Morino & Snell, 1967). The position of Tyr72, the general acid catalyst as shown for analogous Tyr71 in TPL (Chen *et al.*, 1995), can be affected by movement of Glu70 upon monovalent cation binding.

Comparison of Tnase with other PLP enzymes

Alexander *et al.* (1994) divided the PLP-dependent enzymes involved in amino acid metabolism into three regio-specific α , β and γ -families after the substrate carbon on which the leaving group is located and confirmed this by amino acid sequence relationships. They suggested that enzymes within one regio-specific family are evolutionary related and their 3-D structures should be conserved. The authors attributed the α , β -eliminating PLP-dependent lyases (Tnase and TPL) to the α -family. The 3-D structures of D-amino acid aminotransferase (Sugio *et al.*, 1995), catalysing the transamination reaction at the substrate C^2 -position and alanine racemase (Shaw *et al.*, 1997) catalysing the substrate racemization at C^2 position, proved to be completely different from the structure of AATase and between them, implying the existence of at least three non-related subfamilies within the α -family. Additionally, the similarity of the 3-D structure of CBL, which belong to the γ -family to the AATase structure suggests that PLP-dependent enzymes of α - and γ -families are evolutionary related (Clausen *et al.*, 1996). So for convenience of discussion the term "AATase subfamily" of PLP-dependent enzymes will be used. It embraces all PLP-dependent enzymes with the unique topology seven stranded β -sheet of the large domain, which was first discovered in AATase. There are currently six enzymes with known 3-D structure which can be attributed to the AATase subfamily; AATase (Kirsch *et al.*, 1984), TPL (Antson *et al.*, 1993), DGD (Toney *et al.*, 1993), APT (Watanabe *et al.*, 1989), OrnDC (Momany *et al.*, 1995a) and CBL (Clausen *et al.*, 1996). Although the number of subunits in these enzymes varies from two in AATase to 12 in OrnDC, the basic "catalytic unit" of all these enzymes; the AATase-like dimer with the active site at the subunit interface is quite similar to the catalytic dimer of Tnase. Tnase can be attributed to AATase subfamily of PLP enzymes on basis of topology of the β -sheet of its large domain. The secondary structure of the substrate-binding small domains built around the antiparallel β -sheet varies more significantly between Tnase and other enzymes of the AATase subfamily.

Tnase is closely related to another PLP-dependent lyase, TPL, which degrades tyrosine to phenol, ammonia and pyruvate, and performs some other α , β -elimination and β -replacement reactions (Demidkina & Myagkih, 1989). The reaction mech-



Figure 16. Stereo plot of C^α traces of Tnase (thick lines) and TPL in apo form (thin lines; PDB code 1TPL) superimposed using the β -sheets of the large domains. The residues not defined in the TPL structure are not shown for Tnase.

anism of TPL is similar to that of Tnase except that TPL is specific to the phenol side-chain rather than indole. Both tryptophan and tyrosine have bulky aromatic side-chains with heteroatoms (a possible electron sink from the aromatic ring). The enzymes have a high sequence similarity, with 114 conserved residues in six Tnase and three TPL sequences (Figure 5). There are relatively few insertions and deletions between these sequences. The level of sequence identity between different Tnases and TPLs (40% to 50%) is almost the same as between all known Tnases (50% to 60%). The secondary (Figure 16), ternary and quaternary structures are also highly conserved. In Tnase helix $\alpha 4$ is two turns longer than in TPL with an insertion of eight residues at its C terminus.

When the apo TPL and holo Tnase structures are superimposed using the β -sheet of the large domain (Figure 16), the small domain of Tnase is rotated 9° towards the large one resulting in a more closed subunit conformation, with some parts of the small domain being displaced by up to 6 Å. This seems to reflect the difference between apo and holo enzymes. Closure of the Tnase subunit upon PLP binding is supported by sedimentation studies (Snell, 1975) which suggest that a large conformational change accompanies binding of PLP by apo Tnase.

Most residues involved with cofactor binding in Tnase are conserved in TPL, the only exception being Ala225 on which the PLP pyridine ring lies in Tnase. In TPL it is substituted by Thr. As in Tnase, only one monovalent cation site has been identified by studying complexes of apo TPL with Cs^+ and K^+ (Antson *et al.*, 1994). The structure of the K^+ binding site in Tnase is very similar to the structure of the monovalent cation site in TPL, with all residues and water molecules involved in monovalent cation binding being conserved.

Owing to the high similarity of the 3-D structures of Tnase and TPL, many conclusions drawn from comparison of TPL with other PLP-dependent enzymes are valid for Tnase. As the second-

ary structure comparison of TPL with AATase has already been done (Antson *et al.*, 1992, 1993), the comparison between Tnase and chicken heart mitochondrial AATase (McPhalen *et al.*, 1992; PDB code 7AAT) will be limited mainly to the PLP-binding site. AATase was chosen for comparison as its structure and catalytic mechanism are the most studied among PLP-dependent enzymes and most of them have been thoroughly compared with AATase (Antson *et al.*, 1993; Toney *et al.*, 1995; Sugio *et al.*, 1995; Momany *et al.*, 1995b; Clausen *et al.*, 1996).

Many residues involved in PLP binding are structurally conserved between Tnase and AATase (Figure 17; Table 2). Phe132, which in Tnase forms a stacking pair with the PLP pyridine ring from the solution side is replaced in AATase by Trp140. Arg101 which contributes its guanidinium group to salt bridge formation with the PLP phosphate group is replaced by Thr109. The PLP phosphate ion pairing guanidinium group in AATase is provided by Arg266. The conformations about the phosphate ester bond for PLP phosphate are significantly different between Tnase and AATase from chicken heart mitochondria (Figure 17). There is a 90° difference in torsion angle along the bond C5–C5' and 40° difference in torsion angle along the bond C5'–O4 between the two enzymes. Thus the PLP phosphate group is located above the PLP pyridine ring in chicken mitochondrial AATase and below the ring in Tnase. This could contribute to a different pH dependence of protonation state of PLP phosphate between the two enzymes (Mattingly *et al.*, 1982; Schnakerts & Snell, 1983). Similar differences in conformations about the phosphate ester bond for PLP phosphate group between pig cytosolic AATase and chicken mitochondrial AATase has been discussed by Arnone *et al.* (1985).

There are two significant differences in the nature of PLP binding between Tnase and AATase. While in Tnase PLP O3' makes a salt bridge with the positively charged guanidinium group of

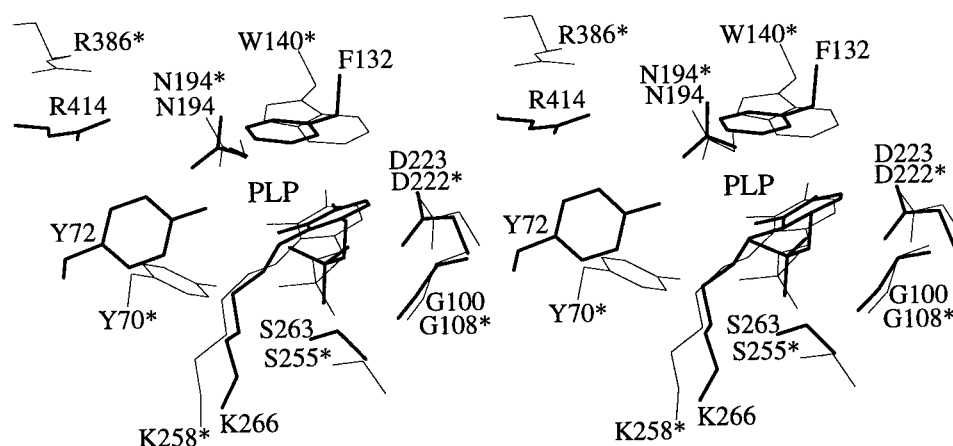


Figure 17. Superposition of the active sites of Tnase (thick lines) and the PLP form of AATase from chicken heart mitochondria at pH 7.5 (PDB code 7AAT; thin lines). The conserved residues or those with similar functions are shown. The AATase residues are marked with an asterisk.

Arg226 and a salt bridge/hydrogen bond with the imine NZ of Lys266, PLP O3' in AATase makes a salt bridge only with the aldimine nitrogen, as Tyr225 which is H-bonded to it carries no charge in the catalytic pH range. This should provide a different pK_A of the Schiff's base and give a different ratio of internal aldimine species between the two enzymes (Hayashi *et al.*, 1993). The other difference is that in Tnase Asp223, coordinating PLP N1, is H-bonded to the uncharged Thr135 while the equivalent Asp222 in AATase is H-bonded to the His143. Protonation of His143 in AATase could lower the pK_A of PLP N1, although NMR spectra show that His143 is not protonated at a pH above 5 (Mollova *et al.*, 1997).

Comparison of the Tnase PLP-binding site with those of TPL, AATase, DGD, OrnDC, APT and CBL reveals only two conserved enzyme-cofactor interactions. They are: the Schiff's base of PLP C4' with NZ of the active site lysine and an aspartate which makes a salt bridge/hydrogen bond with

PLP N1. The serine located three residues before the active site lysine in the motif Ser-X-X-Lys(PxI) is conserved in TPL, AATase, DGD, APT and OrnDC, but is replaced by alanine in CBL. It is conserved in another γ -eliminating enzyme; rat cystathionine γ -lyase (Clausen *et al.*, 1996). Preliminary data on a quinonoid complex of Tnase (Isupov *et al.*, unpublished results) suggest that this serine forms a H-bond with the active site lysine in the external aldimine and/or quinonoid steps of the reaction, when the latter is not involved in a Schiff's base with the cofactor.

The binding of the PLP phosphate at the N terminus of a long α -helix and the position of the PLP pyridine ring between the stacking side-chain on the solution side and the side-chain of Ala or Thr on the protein side are structurally conserved in all the above enzymes. The stacking interaction may be important for proper orientation of the PLP pyridine ring and increase of the electrophilic character of the conjugated PLP system, although the

Table 2. Comparison of critical amino acid residues in *P. vulgaris* Tnase and chicken heart mitochondrial AATase active sites

Functional or structural role	Tnase	AATase ^a
Schiff's base with PLP	Lys266	Lys258
Salt bridge/H-bond to PLP N1	Asp223	Asp222
H-bond to Asp223 and Asp222, respectively	Thr135	His143
Salt bridge/H-bond to PLP O3'	Arg226	Tyr225
H-bond to PLP O3'	Asn194	Asn194
Salt bridge/H-bond with substrate α -carboxylate group	Arg414	Arg386
Stacking interaction with PLP pyridine ring	Phe132	Trp140
Supporting PLP pyridine ring from protein side	Ala225	Ala224
Interactions with PLP phosphate	Gln99	Ser107
	Gly100	Gly108
	Arg101	Thr109
	Ser263	Ser255
	-	Arg266
	Tyr72' ^b	Tyr70'
	Tyr301'	Asn297'

^a Residues numbered according to chicken mitochondrial AATase.

^b Primed (') numbers refer to residues from neighbouring subunit in catalytic dimer.

type of stacking residue seems not to be crucial as all possible aromatic residues occur; Phe132 in Tnase, Phe123 in TPL, Trp140 in AATase, Trp138 in DGD, Tyr152 in APT, Tyr111 in CBL and His223 in OrnDC.

The dual role of Tyr71 in TPL (Tyr72 in Tnase) as general acid catalyst in the elimination of leaving group from the quinonoid intermediate and in PLP binding has been shown by Chen *et al.*, (1995). Toney & Kirsch (1991) have shown that the equivalent Tyr70 in AATase has only a PLP binding role. This is consistent with the absence of any residue analogous to Tyr72 in OrnDC (Momany *et al.*, 1995a).

While catalytic dimers in Tnase are held in a tetramer by a hydrophobic cluster in the centre of the molecule (Figure 9) and intersubunit β -sheets at the edge of the molecule (Figure 6(c)), CBL dimers associate into a tetramer by ionic interactions in the centre of the tetramer (Figure 5 in Clausen *et al.*, 1996). The notable distinction between the principles of tetramer formation in DGD, APT and TPL (Toney *et al.*, 1995) is also valid for Tnase. While in DGD the N terminus is involved in stabilisation of the catalytic dimer as in AATase, in Tnase and TPL it is involved in the tetramer interface. The interface between the two catalytic dimers in DGD is at the "bottom" of the dimer, while in Tnase and TPL the interface interactions are at the "top" of the dimer.

DGD activity is dependent on the presence of monovalent cations and two monovalent cation sites per subunit were identified in its structure (Toney *et al.*, 1993), one with higher affinity for K^+ and a second with higher affinity for Na^+ . Although the positions of both ion binding sites in the DGD subunit are quite different and not located at the subunit interface as in Tnase, there are some similarities between the sites. First the DGD sites are not located in the active site and do not participate directly in catalytic reaction, but rather provide the required alignment of protein catalytic groups. Secondly, only oxygens are ligands to the cations. The K^+ in DGD has only six ligands, while in Tnase it has seven, although the distance K^+ -Glu70 O (3.37 Å) in Tnase is longer than the average distance from K^+ to the other six ligands (2.83 Å). In DGD the average distance between K^+ and its six ligands is even shorter (2.73 Å).

Tryptophan synthase is currently the only representative of the regio-specific β -family of PLP enzymes (Alexander *et al.*, 1994) for which the 3-D structure is known (Hyde *et al.*, 1988). Tnase and the β_2 dimer of tryptophan synthase $\alpha_2\beta_2$ complex catalyse the same β -replacement reaction, synthesis of tryptophan from serine and indole. However, as shown originally for TPL (Antson *et al.* 1992, 1993) the secondary structure and active site organisation in β -subunit of tryptophan synthase are quite different from those of Tnase. Superposition of β -subunit tryptophan synthase (PDB code 1WSY) and Tnase using the plane of the PLP ring revealed

no similarities in the mode of PLP binding (data not shown). The residues involved in PLP binding are different in the two structures and are located on different secondary structure elements, suggesting that there is no evolutionary relationship between Tnase and the β -subunit of tryptophan synthase. Binding of K^+ and Cs^+ to $\alpha_2\beta_2$ tryptophan synthase complex has been described recently by Rhee *et al.* (1996). There appears to be no structural similarity between monovalent cation binding site in Tnase and either of the tryptophan synthase sites, besides the facts that both in Tnase and tryptophan synthase the monovalent cations are not located in the active site and have only oxygen ligands.

The structures of glycogen phosphorylase (Weber *et al.*, 1978; Barford & Johnson, 1989), D-amino acid aminotransferase (Sugio *et al.*, 1995) and alanine racemase (Shaw *et al.*, 1997) have no significant structural homology to Tnase at the secondary structural level or in the active site.

The results reported herein form the basis for future investigations on the structure function relationships of tryptophanase, including the analysis of inhibitor complexes, different monovalent cations complexes and site-directed mutagenesis.

Methods

Crystallisation and data collection

Tnase was produced from recombinant cells of *E. coli* SWS370 containing the Tnase operon of *P. vulgaris* in plasmid pAVK2 (Kamath & Yanofsky, 1992). Cells were grown under conditions described by Phillips and Gollnick (1989) with the following modification: the medium was supplemented with DL-1-methyltryptophan (5 mg/l) to induce Tnase synthesis (Kamath & Yanofsky, 1992). The enzyme was isolated as described by Zakomirdina *et al.* (1989) with an additional fast protein liquid chromatography step. The Tnase was applied to an anion exchange column (MonoQ HR 5/5, Pharmacia) equilibrated with 0.05 M potassium phosphate (pH 7.7), containing 1 mM EDTA, 2 mM DTT, 0.04 mM PLP and eluted with a linear 0 to 0.4 M KCl gradient in the same buffer. Crystallisation has been previously reported (Dementieva *et al.*, 1994). The crystals were grown by the hanging drop technique in the presence of 0.25 mM PLP, 5 mM DTT and 0.1 M CsCl in 0.1 M potassium phosphate buffer (pH 7.8), with 27% PEG 4000. The space group was determined as $P2_12_12_1$ with cell dimensions $a = 115.0$ Å, $b = 118.2$ Å, $c = 153.7$ Å. The asymmetric unit contains a tetramer with molecular mass 208 kDa, giving a specific volume of 2.49 Å³/Da and a solvent content of 51% (Matthews, 1968).

Initially 2.5 Å native data were collected using a rotating anode generator and Raxis image plate detector as described previously (Dementieva *et al.*, 1994). The data were 90.5% complete and reduced

Table 3. Statistics of the synchrotron diffraction data

Resolution ranges	$\langle I \rangle$	$\langle I/\sigma(I) \rangle$	Redundancy	$R_{\text{merge}}\%$ ^a	Completeness	
					% > 3 σ	
18.00–4.50	2975.2	20.1	5.63	6.9	97.2	93.8
4.50–3.58	3060.7	21.6	6.01	9.3	98.5	93.6
3.58–3.13	1719.3	15.6	3.70	8.5	97.4	86.3
3.13–2.85	998.3	10.7	2.60	8.8	97.6	78.6
2.85–2.64	695.2	8.1	2.57	11.5	97.7	70.4
2.64–2.49	566.1	6.8	2.55	13.8	97.7	65.6
2.49–2.36	493.3	5.8	2.54	15.9	97.7	60.9
2.36–2.26	454.3	5.1	2.52	19.9	97.4	55.1
2.26–2.17	387.3	4.0	2.51	23.7	97.3	50.9
2.17–2.10	345.4	3.2	2.49	27.3	97.3	46.8
Total	1183.2	11.0	3.33	9.8	97.6	70.0

^a $R_{\text{merge}} = \sum |I - \langle I \rangle| / \sum I$, where I is the intensity of reflection.

with an $R_{\text{merge}} = |I - \langle I \rangle| / I$ of 8.2%. Subsequently new native data to 2.1 Å resolution were collected at 8°C at a wavelength of 0.95 Å on the EMBL BW7B wiggler beam line, at DESY, Hamburg using a Marresearch image plate scanner. The data were processed with DENZO and SCALEPACK (Otwinowski & Minor, 1997). 397510 individual measurements were reduced to 117863 unique reflections with an overall R_{merge} of 9.8% (Table 3). The data are 97.6% complete.

Structure determination and refinement

The structure was solved by molecular replacement (MR) using the full atomic model of apo TPL from *C. freundii* (Antson *et al.*, 1993; PDB code 1TPL). The level of sequence identity between Tnase and TPL is 50%. The cross-rotation function with integration radius of 30 Å and translation function (Crowther & Blow, 1967) were calculated in the resolution range 10 to 4 Å using AMORE (Navaza, 1994). No MR solution was found using one TPL subunit as a search model, presumably due to the large relative movement of domains within the subunit. However, the catalytic dimer of TPL gave clear MR solutions, as relative positions of subunits in the catalytic dimer were conserved between TPL and Tnase. As the asymmetric unit of the Tnase crystals contains a tetramer, two MR solutions had to be found for a dimer model. The rotation peaks were 10.4 and 10.1 σ for the two solutions, the next peak was 8.6 σ . The translation solutions had correlations $C = \sum (|F_o| - \langle |F_o| \rangle)(|F_c| - \langle |F_c| \rangle) / (\sum (|F_o| - \langle |F_o| \rangle)^2 \sum (|F_c| - \langle |F_c| \rangle)^2)^{1/2}$ of 15.2% and 18.2% and R -factors $R = \sum ||F_o| - |F_c|| / \sum |F_o|$ of 55.2% and 54.1%, respectively. Correlations for wrong peaks of translation function were below 12.5%. With one dimer fixed the solution found for the other had an R -factor of 52.3% and a correlation of 25.9%.

Refinement was conducted using PROLSQ (Hendrickson & Konnert, 1980) implemented in the CCP4 program suite (CCP4, 1994). The measured reflections in the resolution range of 10 to 2.1 Å

with no σ cutoff were used excluding 2.0% randomly distributed reflections assigned to calculate R_{free} . Individual atomic B -factors were refined at all stages. The phases were improved by four-fold NCS averaging (Bricogne, 1974) of $(2F_o - F_c)$ using RAVE (Jones; 1992). A representative section of the averaged electron density is shown in Figure 12. Manual correction of the model was performed on an Evans and Sutherland workstation using FRODO (Jones, 1985) and O (Jones *et al.*, 1991). Rebuilding was performed independently for each subunit. Four PLP molecules and four potassium ions were identified. Water molecules were added using ARP (Lamzin & Wilson, 1993). Initially the refinement was conducted without NCS restraints. This allowed identification of the regions of the model with high deviation from NCS symmetry. Further refinement was performed with NCS restraints. Separate NCS operations were used for small and large domains of different subunits. The lowest value of R_{free} (Brünger, 1992) was achieved when strict NCS restraints were imposed on main and side-chains of the large domain residues and strict, medium or no NCS restraints on different parts of small domains. For further improvement the model has been refined against data at 18 to 2.1 Å resolution by maximum likelihood method as implemented in REFMAC (Murshudov *et al.*, 1997).

Acknowledgements

We thank Garib Murshudov and Tatyana Demidkina for useful discussions, Martin Singleton for helpful comments on the manuscript, Galya Obmolova and Sergei Strelkov for the help with crystal preparation. The research was supported in part by the NATO Collaborative Research Grants Programme (grant GRG920962), SERC (UK), INTAS grant 1010-CT93-0012, grant of Howard Hughes Medical Institute 75195-540001, the Russian Foundation for Fundamental Research grant 96-04-49851 and the International Science Foundation grant M52000.

References

- Alexander, F. W., Sandmeier, E., Mehta, P. K. & Christen, P. (1994). Evolutionary relationships among pyridoxal 5'-phosphate-dependent enzymes. Regio-specific α , β , and γ families. *Eur. J. Biochem.* **219**, 953–960.
- Antson, A. A., Strokopytov, B. V., Murshudov, G. N., Isupov, M. N., Harutyunyan, E. H., Demidkina, T. V., Vassilyev, D. G., Dauter, Z., Terry, H. & Wilson, K. S. (1992). The polypeptide chain fold in tyrosine phenol-lyase, a pyridoxal 5'-phosphate-dependent enzyme. *FEBS Letters*, **302**, 256–260.
- Antson, A. A., Demidkina, T. V., Gollnick, P., Dauter, Z., Von Tersch, R. L., Long, J., Berezhnoy, S. N., Phillips, R. S., Harutyunyan, E. H. & Wilson, K. S. (1993). Three-dimensional structure of tyrosine phenol-lyase. *Biochemistry*, **32**, 4195–4206.
- Antson, A. A., Dodson, G. G., Wilson, K. S., Pletnev, S. V., Harutyunyan, E. G. & Demidkina, T. V. (1994). Crystallographic studies of tyrosine phenol-lyase. In *Biochemistry of Vitamin B₆ and PQQ* (Marino, G., Sannio, G. & Bossa, F., eds), pp. 187–191, Birkhauser, Basel Switzerland.
- Arnone, A., Rogers, P. H., Hyde, C. C., Briley, P. D., Metzler, C. M. & Metzler, D. E. (1985). Pig cytosolic aspartate aminotransferase: the structures of internal aldimine, external aldimine and ketimine and of the β subform. In *Transaminases* (Christen, P. & Metzler, D. E., eds), pp. 138–155, Wiley, New York.
- Barford, D. & Johnson, L. N. (1989). The allosteric transition of glycogen phosphorylase. *Nature*, **240**, 609–616.
- Bernstein, F. C., Koetzle, T. F., Williams, G. J. B., Meyer, E. J., Brice, M. D., Rogers, J. K., Kennard, O., Shimanouchi, T. & Tasumi, M. (1977). The protein data bank: a computer-based archival file for macromolecular structures. *J. Mol. Biol.* **112**, 535–542.
- Borisov, V. V., Borisova, S. N., Sosfenov, N. I. & Vainstein, B. K. (1980). Electron density map of chicken heart cytosol aspartate transaminase at 3.5 Å resolution. *Nature*, **284**, 189–190.
- Boyer, P. D., Lardy, H. A. & Phillips, P. H. (1942). The role of potassium in muscle phosphorylations. *J. Biol. Chem.* **146**, 673–680.
- Braunstein, A. E. & Shemyakin, M. M. (1953). The theory of processes of amino acid metabolism catalysed by pyridoxal 5'-phosphate-dependent enzymes. *Biokhimiya*, **18**, 393–411 (in Russian).
- Bricogne, G. (1974). Geometric sources of redundancy in intensity data and their use for phase determination. *Acta Crystallog. sect. A*, **30**, 395–405.
- Brünger, A. (1992). Free R value: a novel statistical quantity for assessing the accuracy of crystal structures. *Nature*, **355**, 472–475.
- Chen, H. Y., Demidkina, T. V. & Phillips, R. S. (1995). Site-directed mutagenesis of tyrosine-71 to phenylalanine in *Citrobacter freundii* tyrosine phenol-lyase: evidence for dual roles of tyrosine-71 as a general acid catalyst in the reaction mechanism and in cofactor binding. *Biochemistry*, **34**, 12276–12283.
- Clausen, T., Huber, R., Laber, B., Pohlenz, H. & Messerschmidt, A. (1996). Crystal structure of the pyridoxal-5'-phosphate dependent cystathionine β -lyase from *Escherichia coli* at 1.83 Å. *J. Mol. Biol.* **262**, 202–224.
- Collaborative Computational Project No 4 (1994). The CCP4 suite: programs for protein crystallography. *Acta Crystallog. sect. D*, **50**, 760–763.
- Cowell, J. L., Moser, K. & DeMoss, R. D. (1973). Tryptophanase from *Aeromonas liquefaciens*. Purification, molecular weight and some chemical, catalytic and immunochemical properties. *Biochim. Biophys. Acta*, **315**, 449–463.
- Crowther, R. A. & Blow, D. M. (1967). A method of positioning a known molecule in an unknown crystal structure. *Acta Crystallog.* **23**, 544–548.
- Cruickshank, D. W. J. (1996). Protein precision re-examined: Luzzati plots do not estimate final errors. In *Macromolecular refinement* (Dodson, E., Moore, M., Ralph, A. & Bailey, S., eds), pp. 11–22, CCLRC Daresbury Laboratory, Warrington UK.
- Deeley, M. C. & Yanofsky, C. (1981). Nucleotide sequence of structural gene for tryptophanase of *Escherichia coli* K-12. *J. Bacteriol.* **147**, 787–796.
- Dementieva, I. S., Zakomirdina, L. N., Sinitzina, N. I., Antson, A. A., Wilson, K. S., Isupov, M. N., Lebedev, A. A. & Harutyunyan, E. H. (1994). Crystallization and preliminary X-ray investigation of holotryptophanases from *Escherichia coli* and *Proteus vulgaris*. *J. Mol. Biol.* **235**, 783–786.
- Demidkina, T. V. & Myagkih, I. V. (1989). The activity and reaction specificity of tyrosine phenol-lyase regulated by monovalent cations. *Biochimie*, **71**, 565–571.
- DeMoss, R. D. & Moser, K. (1969). Tryptophanase in diverse bacterial species. *J. Bacteriol.* **98**, 167–171.
- Dunathan, H. C. (1966). Conformation and reaction specificity in pyridoxal phosphate enzymes. *Proc. Natl Acad. Sci. USA*, **55**, 712–716.
- Evans, H. J. & Sorger, J. (1966). Role of mineral elements with emphasis on univalent cations. *Annu. Rev. Plant. Physiol.* **17**, 47–76.
- Ford, J. C., Eichele, G. & Jansonius, J. N. (1980). Three-dimensional structure of a pyridoxal-phosphate-dependent enzyme, mitochondrial aspartate aminotransferase. *Proc. Natl Acad. Sci. USA*, **77**, 2559–2563.
- GCG, (1994). *Program Manual for the Wisconsin Package, Version 8*, Genetics computer group, Madison WI.
- Gopinatham, K. P. & DeMoss, R. D. (1966). Reversible dissociation of tryptophanase into protein subunits. *Proc. Natl Acad. Sci. USA*, **56**, 1223–1225.
- Harutyunyan, E. G., Malashkevich, V. N., Tersyan, S. S., Kochkina, V. M., Torchinsky, Yu. M. & Braunstein, A. E. (1982). 3-Dimensional structure at 3.2 Å resolution of the complex of cytosolic aspartate-aminotransferase from chicken heart with 2-oxoglutarate. *FEBS Letters*, **138**, 113–116.
- Hayashi, H., Wada, H., Yoshimura, T., Esaki, N. & Soda, K. (1993). Recent topics in pyridoxal-phosphate enzymes studies. *Annu. Rev. Biochem.* **59**, 87–110.
- Hendrickson, W. A. & Konnert, J. H. (1980). Incorporation of stereochemical information into crystallographic refinement. In *Computing in Crystallography* (Diamond, R., Ramaseshan, S. & Venkatesan, K., eds), pp. 13.01–13.23, Indian Academy of Sciences, Bangalore.
- Hirahara, T., Suzuki, S., Horinouchi, S. & Beppu, T. (1992). Cloning, nucleotide sequences and overexpression in *Escherichia coli* of tandem copies of a tryptophanase gene in an obligately symbiotic thermophile, *Symbiobacterium thermophilum*. *Appl. Environ. Microbiol.* **58**, 2633–2642.

- Hirahara, T., Horinouchi, S. & Beppu, T. (1993). Cloning, nucleotide-sequence, and overexpression in *Escherichia coli* of the β -tyrosinase gene from an obligately symbiotic thermophile, *Symbiobacterium thermophilum*. *Appl. Microbiol. Biotechnol.* **39**, 341–346.
- Hoch, S. O. & DeMoss, R. D. (1973). Catalytic studies on tryptophanase from *Bacillus alvei*. *J. Bacteriol.* **114**, 341–350.
- Hogberg-Raibaud, A., Raibaud, O. & Goldberg, M. E. (1975). Kinetic and equilibrium studies on the activation of *Escherichia coli* K12 tryptophanase by pyridoxal 5'-phosphate and monovalent cations. *J. Biol. Chem.* **250**, 3352–3358.
- Hyde, C. C., Ahmed, S. A., Padlan, E. A., Miles, E. W. & Davies, D. R. (1988). Three-dimensional structure of the tryptophan synthase $\alpha_2\beta_2$ multienzyme complex from *Salmonella typhimurium*. *J. Biol. Chem.* **263**, 17857–17871.
- Iwamori, S., Yoshino, S., Ishiwata, K. I. & Makiguchi, N. (1991). Structure of tyrosine phenol-lyase genes from *Citrobacter freundii* and structural comparison with tryptophanase from *Escherichia coli*. *J. Ferment. Bioeng.* **72**, 147–151.
- Ivanov, V. I. & Karpeisky, M. Y. (1969). Dynamic three-dimensional model for enzymatic transamination. *Advan. Enzymol.* **32**, 21–53.
- Iwamori, S., Oikawa, T., Ishiwata, K. I. & Makiguchi, N. (1992). Cloning and expression of the *Erwinia herbicola* tyrosine phenol-lyase gene in *Escherichia coli*. *Biotechn. Appl. Biochem.* **16**, 77–85.
- Jones, T. A. (1985). Interactive computer graphics: FRODO. *Methods Enzymol.* **115**, 157–171.
- Jones, T. A., Zou, J.-Y., Cowan, S. W. & Kjeldgaard, M. (1991). Improved methods for building protein models in electron density maps and the location of errors in these models. *Acta Crystallog. sect. A*, **47**, 110–119.
- Jones, T. (1992). A, yaap, asap, @#*? A set of averaging programs. In *Molecular Replacement* (Dodson, E. J., ed.), pp. 91–105, SERC Daresbury Laboratory, Warrington UK.
- June, D. S., Suelter, C. H. & Due, J. L. (1981a). Kinetics of pH-dependent interconversion of tryptophanase spectral forms studied by scanning stopped-flow spectrophotometry. *Biochemistry*, **20**, 2707–2713.
- June, D. S., Suelter, C. H. & Due, J. L. (1981b). Equilibrium and kinetic study of interaction of amino acid inhibitors with tryptophanase: mechanism of quinonoid formation. *Biochemistry*, **20**, 2714–2719.
- Kamath, A. V. & Yanofsky, C. (1992). Characterization of the tryptophanase operon of *Proteus vulgaris*. Cloning, nucleotide sequence, amino acid homology, and *in vitro* synthesis of the leader peptide and regulatory analysis. *J. Biol. Chem.* **267**, 19978–19985.
- Kamitori, S., Hirotsu, K., Higuchi, T., Kondo, K., Inoue, K., Kuramitsu, S., Kagamiyama, H., Higuchi, Y., Yasuoka, N., Kusunoki, M. & Matsuura, Y. (1988). Three-dimensional structure of aspartate aminotransferase from *Escherichia coli* at 2.8 Å resolution. *J. Biochem. (Tokyo)*, **104**, 317–318.
- Kawasaki, I. K., Yokota, A., Oita, A., Kobayashi, C., Yoshikawa, S., Kawamoto, S. I., Takao, S. & Tomita, F. (1993). Cloning and characterization of tryptophanase gene from *Enterobacter aerogenes* SM-18. *J. Gen. Microbiol.* **139**, 3275–3281.
- Kawata, Y., Tani, S., Sato, M., Katsube, Y. & Tokushige, M. (1991). Preliminary X-ray crystallographic analysis of tryptophanase from *Escherichia coli*. *FEBS Letters*, **284**, 270–272.
- Kirsch, J. F., Eichele, G., Ford, G. C., Vincent, M. G. & Jansonius, J. N. (1984). Mechanism of action of aspartate aminotransferase on the basis of its spatial structure. *J. Mol. Biol.* **174**, 497–525.
- Koostra, P. J., Kalk, K. H. & Hol, W. G. J. (1988). Soaking in Cs_2SO_4 reveals a caesium–aromatic interaction in bovine-liver rhodanese. *Eur. J. Biochem.* **177**, 345–349.
- Kraulis, P. J. (1991). MOLSCRIPT: a program to produce both detailed and schematic plots of protein structures. *J. Appl. Crystallog.* **24**, 946–950.
- Lamzin, V. S. & Wilson, K. S. (1993). Automated refinement of protein models. *Acta Crystallog. sect. D*, **49**, 129–147.
- Laskowski, R. A., MacArthur, M. W., Moss, D. S. & Thornton, J. M. (1993). PROCHECK: a program to check the stereochemical quality of protein structures. *J. Appl. Crystallog.* **26**, 283–291.
- Laskowski, R. A., MacArthur, M. W. & Thornton, J. M. (1994). Evaluation of protein coordinate data sets. In *From First Map to Final Model* (Bailey, S., Hubbard, R. & Waller, D., eds), pp. 149–159, EPSRS Daresbury Laboratory, Warrington UK.
- Lijk, L. J., Trofs, C. A., Kalk, K. H., De Maeyer, M. C. H. & Hol, W. G. J. (1984). Differences in the binding of sulphate, selenate and thiosulphate ions to bovine liver rhodanese, and a description of the binding site for ammonium and sodium ions. An X-ray diffraction study. *Eur. J. Biochem.* **142**, 399–408.
- Malashkevich, V., Strokopytov, B. V., Borisov, V. V., Dauter, Z., Wilson, K. S. & Torchinsky, Y. M. (1995). Crystal structure of the closed form of chicken cytosolic aspartate aminotransferase at 1.9 Å resolution. *J. Mol. Biol.* **247**, 111–124.
- Matthews, B. W. (1968). Solvent content of protein crystals. *J. Mol. Biol.* **33**, 491–497.
- Mattingly, M. E., Mattingly, J. R. & Martinezcarrion, M. (1982). P-31 nuclear magnetic resonance of mitochondrial aspartate aminotransferase: the effects of solution pH and ligand-binding. *J. Biol. Chem.* **257**, 8872–8878.
- McPhalen, C. A., Vincent, M. G. & Jansonius, J. N. (1992). X-ray structure refinement and comparison of three forms of mitochondrial aspartate aminotransferase. *J. Mol. Biol.* **225**, 495–517.
- Melchior, J. B. (1965). The role of metal ions in the pyruvic kinase reaction. *Biochemistry*, **4**, 1518–1525.
- Metzler, D. E., Ikawa, M. & Snell, E. E. (1954). A general mechanism for vitamin B₆-catalyzed reactions. *J. Am. Chem. Soc.* **76**, 648–652.
- Metzler, D. E. (1977). *Biochemistry. The Chemical Reactions of Living Cells*, pp. 270, Academic Press, New York.
- Metzler, C. M., Viswanath, R. & Metzler, D. E. (1991). Equilibria and absorption spectra of tryptophanase. *J. Biol. Chem.* **266**, 9374–9381.
- Miles, E. W. (1986). Pyridoxal phosphate enzymes catalyzing β -elimination and β -replacement reactions. In *Vitamin B₆, Pyridoxal Phosphate, Chemical, Biochemical, and Medical Aspects* (Dolphin, D., Poulson, R. & Avramovic, O., eds), part B, pp. 253–310, Wiley, New York.
- Mollova, E. T., Metzler, D. E., Kintanar, A., Kagamiyama, H., Hayashi, H., Hirotsu, K. & Miyahara, I. (1997). Use of ^1H - ^{15}N heteronuclear multiple-quantum coherence NMR spectroscopy to

- study the active site of aspartate aminotransferase. *Biochemistry*, **36**, 615–625.
- Momany, C., Ernst, S., Ghosh, R., Chang, N. & Hackert, M. L. (1995a). Crystallographic structure of a PLP-dependent ornithine decarboxylase from *Lactobacillus* 30a to 3.0 Å resolution. *J. Mol. Biol.* **252**, 643–655.
- Momany, C., Ghosh, R. & Hackert, L. (1995b). Structural motifs for pyridoxal-5'-phosphate binding in decarboxylases: an analysis based on the crystal structure of the *Lactobacillus* 30a ornithine decarboxylase. *Protein Science*, **4**, 849–854.
- Morino, Y. & Snell, E. E. (1967). The subunit structure of tryptophanase. *J. Biol. Chem.* **242**, 5591–5601.
- Murshudov, G. N., Vagin, A. A. & Dodson, E. J. (1997). Refinement of macromolecular structures by the maximum likelihood method. *Acta Crystallog. sect. D*, **53**, 240–255.
- Murshudov, G. N. & Dodson, E. J. (1997). Simplified error estimation *a la* Cruickshank in macromolecular crystallography. In *CCP4 Newsletter on Protein Crystallography* (Winn, M., ed.), no. 33, pp. 31–39, Daresbury Laboratory, Warrington UK.
- Navaza, J. (1994). AMoRe: an automated package for molecular replacement. *Acta Crystallog. sect. D*, **50**, 157–163.
- Newton, W. A., Morino, Y. & Snell, E. E. (1965). Properties of crystalline tryptophanase. *J. Biol. Chem.* **240**, 1211–1218.
- O'Leary, M. H. & Brummond, W. (1974). pH jump studies of glutamate decarboxylase. *J. Biol. Chem.* **249**, 3737–3745.
- Otwinowski, Z. & Minor, W. (1997). Processing of X-ray diffraction data collected in oscillation mode. *Methods Enzymol.* **276**, 307–326.
- Phillips, R. S. & Gollnick, P. D. (1989). Evidence that cysteine 298 is in the active site of tryptophan indole-lyase. *J. Biol. Chem.* **264**, 10627–10632.
- Phillips, R. S. (1991). Reaction of indole and analogues with amino acid complexes of *Escherichia coli* tryptophan indole-lyase: detection of a new reaction intermediate by rapid-scanning stopped-flow spectrophotometry. *Biochemistry*, **30**, 5927–5934.
- Phillips, R. S., Richter, I., Gollnick, P., Brzovic, P. & Dunn, M. F. (1991). Replacement of lysine 269 by arginine in *Escherichia coli* tryptophan indole-lyase affects the formation and breakdown of quinonoid complexes. *J. Biol. Chem.* **266**, 18642–18648.
- Ramakrishnan, C. & Ramachandran, G. N. (1965). Stereochemical criteria for polypeptide and protein chain conformation. *Biophys. J.* **5**, 909–933.
- Rhee, S., Parris, K. D., Ahmed, A., Miles, E. W. & Davies, D. R. (1996). Exchange of K⁺ or Cs⁺ for Na⁺ induces local and long-range changes in the three-dimensional structure of the tryptophan synthase $\alpha_2\beta_2$ complex. *Biochemistry*, **35**, 4211–4221.
- Richardson, J. S. (1981). The anatomy and taxonomy of protein structure. *Advan. Protein Chem.* **34**, 167–339.
- Schnakerts, K. D. & Snell, E. E. (1983). Phosphorus 31 nuclear magnetic resonance study of tryptophanase. *J. Biol. Chem.* **258**, 4839–4841.
- Shaw, J. P., Petsko, G. A. & Ringe, D. (1997). Determination of the structure of alanine racemase from *Bacillus stearothermophilus* at 1.9-Å resolution. *Biochemistry*, **36**, 1329–1342.
- Simard, C., Mardini, A. & Bordeleau, L. M. (1975a). Propriétés physiques et chimiques des tryptophanases de cinq espèces d'Enterobacteriaceae. *Can. J. Microbiol.* **21**, 828–833.
- Simard, C., Mardini, A. & Bordeleau, L. M. (1975b). Effet du phosphate de pyridoxal sur les tryptophanases de cinq espèces d'enterobacteriaceae. *Can. J. Microbiol.* **21**, 834–840.
- Snell, E. E. (1975). Tryptophanase: structure, catalytic activities, and mechanism of action. *Advan. Enzymol.* **42**, 287–333.
- Suelter, C. H. (1970). Enzymes activated by monovalent cations. *Science*, **168**, 789–795.
- Suelter, C. H. & Snell, E. E. (1977). Monovalent cation activation of tryptophanase. *J. Biol. Chem.* **252**, 1852–1857.
- Sugio, S., Petsko, G. A., Manning, J. M., Soda, K. & Ringe, D. (1995). Crystal structure of a D-amino acid aminotransferase: how the protein controls stereoselectivity. *Biochemistry*, **34**, 9661–9669.
- Suzuki, S., Hirahara, T., Horinouchi, S. & Beppu, T. (1991). Purification and properties of thermostable tryptophanase from an obligatory symbiotic thermophile, *Symbiobacterium thermophilum*. *Agr. Biol. Chem.* **55**, 3059–3066.
- Tokushige, M., Tsujimoto, N., Oda, T., Honda, T., Yumoto, N., Ito, S., Yamamoto, M., Kim, E. H. & Hiragi, Y. (1989). Role of cysteine residues in tryptophanase for monovalent cation-induced activation. *Biochimie*, **71**, 711–720.
- Toney, M. D., Hohenester, E., Cowan, S. W. & Jansonius, J. N. (1993). Dialkylglycine decarboxylase structure: bifunctional active site and alkali metal sites. *Science*, **261**, 756–759.
- Toney, M. D., Hohenester, E., Keller, J. W. & Jansonius, J. N. (1995). Structural and mechanistic analysis of two refined crystal structures of the pyridoxal phosphate dependent enzyme dialkylglycine decarboxylase. *J. Mol. Biol.* **245**, 151–179.
- Toney, M. D. & Kirsch, J. K. (1991). Kinetics and equilibria for the reactions of coenzymes with wild type and Y70E mutant of *Escherichia coli* aspartate aminotransferase. *Biochemistry*, **30**, 7461–7466.
- Toraya, T., Nihira, T. & Fukui, S. (1976). Essential role of monovalent cations in the firm binding of pyridoxal 5'-phosphate to tryptophanase and β -tyrosinase. *Eur. J. Biochem.* **69**, 411–419.
- Watanabe, N., Sakabe, K., Sakabe, N., Higashi, T., Sasaki, K., Aibara, S., Morita, Y., Yonaha, K., Toyama, S. & Fukutani, H. (1989). Crystal-structure analysis of ω -amino acid: pyruvate aminotransferase with a newly developed Weissenberg camera and an imaging plate using synchrotron radiation. *J. Biochem. (Tokyo)*, **105**, 1–3.
- Watanabe, T. & Snell, E. E. (1972). Reversibility of the tryptophanase reaction: synthesis of tryptophan from indole, pyruvate and ammonia. *Proc. Natl Acad. Sci. USA*, **69**, 1086–1090.
- Weber, I. T., Johnson, L. N., Wilson, K. S., Yeates, D. G. R., Wild, D. L. & Jenkins, J. A. (1978). Crystallographic Studies on the Activity of Glycogen Phosphorylase b. *Nature*, **274**, 433–437.
- Wells, C. M. & Di Cera, E. (1992). Thrombin is a Na⁺-activated enzyme. *Biochemistry*, **31**, 11721–11730.
- Woehl, E. U. & Dunn, M. F. (1995). The roles of Na⁺ and K⁺ in pyridoxal phosphate enzyme catalysis. *Coord. Chem. Rev.* **144**, 147–197.
- Yoshida, H., Utagawa, T., Kumagai, H. & Yamada, H. (1974). Purification, crystallization and properties of tryptophanase from *Proteus rettgeri*. *Agric. Biol. Chem.* **38**, 2065–2072.

Zakomirdina, L. N., Sakharova, I. S. & Torchinsky, Yu. M. (1988). Studies on interaction of tryptophanase

with substrate analogues. *Mol. Biol.* **22**, 187–194 (in Russian).

Edited by K Nagai

(Received 8 July 1997; received in revised form 17 November 1997; accepted 1 December 1997)